HAYATI
Journal of Biosciences

Vol. 32 No. 4, July 2025 920-930
DOI:10.4308/hjb.32.4.920-930
ISSN: 1978-3019
EISSN: 2086-4094

Research Article

The Effect of Papaya Derived Exosome-like Nanoparticle as a Potential Photoprotective Agent in Nanocosmetics

Faticha Nasharo Qisthia Farid, Anggraini Barlian[1*], Indra Wibowo

School of Life Science and Technology, Bandung Institute of Technology, Bandung 40132, Indonesia

ARTICLE INFO

Article history:
Received November 7, 2024
Received in revised form February 16, 2025
Accepted March 5, 2025

KEYWORDS:
fibroblast,
papaya,
PDEN,
photoaging,
UVB,
zebrafish

ABSTRACT

Indonesia, as a tropical nation, experiences year-round ultraviolet radiation exposure. Excessive ultraviolet radiation, particularly UVB, accelerates premature skin aging, known as photoaging. UVB radiation induces photoaging by damaging DNA and increasing the production of reactive oxygen species (ROS), which leads to oxidative stress and results in increased apoptosis, melanogenesis, senescence, cell cycle arrest, and reduced cell migration capacity. Thus, identifying agents that can mitigate photoaging is crucial for developing skincare therapies. One of the alternative therapies currently being developed is plant-derived exosome-like nanoparticles (PDENs). Papaya (*Carica papaya*), renowned for its flavonoid and phenolic content, exhibits potent antioxidant properties and has been extensively utilized in skincare formulations. Therefore, this study investigates the effects of papaya-derived exosome-like nanoparticles (CP-PDEN) on inhibiting photoaging in 1BR3 fibroblast cell lines and zebrafish. Results indicated that CP-PDEN effectively internalized into 1BR3 cells and was categorized as nontoxic. The study then examined photoprotective effects after UVB irradiation (100 mJ/cm^2) and found that CP-PDEN treatment resulted in better viability and nuclear morphology. Furthermore, CP-PDEN accelerates wound closure in 1BR3 cells and decreases melanocyte count in zebrafish compared with controls. In conclusion, CP-PDEN significantly enhanced cell viability and migration and suppressed melanogenesis, indicating its potential for anti-photoaging skincare applications.

1. Introduction

Indonesia, as a tropical country, is exposed to ultraviolet radiation (UVR) throughout the year, which increases the risk of photoaging, a condition characterized by premature skin aging due to UVR. Unlike chronological aging, which is driven by the gradual decline of physiological functions with age, photoaging is highly dependent on the frequency and intensity of UV exposure. UVB radiation, in particular, has been shown to be 70% more potent in inducing photoaging compared to UVA because it not only increases the production of reactive oxygen species (ROS) but also directly damages DNA by forming cyclobutene pyrimidine dimers (CPD) and pyrimidine (6-4) pyrimidone photoproducts (6-4 PP) (Pandel *et al*. 2013). The accumulation of these products triggers oxidative stress, leading to cellular changes such as increased apoptosis, melanogenesis, senescence, and cell cycle arrest. Clinically, prolonged photoaging manifests as skin discoloration, wrinkles, and loss of elasticity (Calvo *et al*. 2024).

One promising approach in dermatological therapy involves the use of plant-derived exosome-like nanoparticles (PDENs), defined as vesicles containing

* Corresponding Author
E-mail Address: aang@itb.ac.id

bioactive compounds isolated from plants (Sall & Flaviu 2023). PDENs are particularly advantageous as therapeutic agents due to their nanoscale size, high biocompatibility, and low immunogenicity (Yi *et al*. 2023). Moreover, compared to mammalian-derived exosomes (MDE), which have been extensively studied, PDENs present a more cost-efficient alternative with higher yields of exosomes (Sarasati *et al*. 2023).

Papaya (*Carica papaya*) has been widely utilized in traditional medicine globally, with numerous studies highlighting its antioxidant and anti-inflammatory properties attributed to secondary metabolites such as flavonoids and phenolic acids (Kong *et al*. 2021). A previous study on *Carica papaya*-plant derived exosome-like nanoparticles (CP-PDEN) also has reported their antioxidant potential, mediated by bioactive compounds like 4H-pyran-4-one-2,3-dihydro-3,5-dihydroxy-6-methyl and maltol (Iriawati *et al*. 2024). Therefore, this study aims to evaluate the potential of *Carica papaya*-plant-derived exosome-like nanoparticles (CP-PDEN) as an alternative therapeutic agent for inhibiting photoaging effects in both in vitro and in vivo models.

2. Materials and Methods

2.1. Isolation of CP-PDEN

The isolation of CP-PDEN from papaya (*Carica papaya*) pulp was performed according to Iriawati *et al*. (2024) using differential centrifugation and precipitation with polyethylene glycol 6000 (PEG6000). Ripe papaya fruit was peeled and ground using a juicer. The obtained juice was then filtered through nylon mesh with pore sizes of 100 µm and 40 µm. The filtrate was then incubated with 30 ppm enzyme pectolyase Y-23 (Seishin Pharmaceutical Co., LTD., Japan) in an incubator shaker at 120 rpm for 90 min at room temperature. The juice was then mixed with an equal volume of aquabidest 1:1 v/v (Ikapharmindo, Indonesia). The mixture was then subjected to serial centrifugation steps at 2000×g for 10 min, 6000×g for 20 min, and 10000×g for 40 min, all at 4°C. The obtained supernatant was mixed with 0.2 M NaCl (Sigma-Aldrich, USA) and 50% PEG 6000 (Himedia, India) to a final concentration of 15% (v/v) and incubated overnight at 4°C. After incubation, the supernatant was centrifuged again at 8000×g for 30 minutes at 4°C, and the pellet was resuspended in aquabidest with 25 mM trehalose (Sigma-Aldrich, USA). The solution was then filtered using syringe filters (Minisart Sartorius, Germany) with pore sizes of 0.45 µm and 0.22 µm and stored at -20°C.

2.2. Characterization of CP-PDEN

The physical characteristics of CP-PDEN were analyzed by evaluating their particle size, zeta potential, and morphology. CP-PDEN particle size and zeta potential characterization were performed with dynamic light scattering (DLS) method using a Nano Particle Analyzer (Horiba SZ-100), while morphological characterization was conducted using a Transmission Electron Microscope (TEM HT7700).

2.3. Protein Concentration of CP-PDEN

Protein concentration of CP-PDEN was measured using the bicinchoninic acid (BCA) assay kit (Thermo Fisher Scientific, USA). Standard solutions were prepared by diluting bovine serum albumin (BSA) ampoule, and the working reagent was prepared by mixing BCA Reagent A and BCA Reagent B (50:1). Subsequently, 25 µL CP-PDEN samples and BSA standard solutions were added to a 96-well plate, followed by 200 µL BCA working reagent in triplicate. The plate was incubated for 30 minutes at 37°C, and absorbance was measured at a wavelength of 595 nm.

2.4. Cell Culture

1BR3 human fibroblast cell lines were purchased from the European Collection of Authenticated Cell Cultures (ECACC) (Salisbury, UK, catalog No: 90011801). The cell lines were cultured in T-25 cell culture flasks with complete Dulbecco's modified essential medium-low glucose (DMEM LG) (Sigma-Aldrich, USA) supplemented with 15% (v/v) fetal bovine serum (FBS) and 1% (v/v) antibiotic-antimycotic (Gibco, USA). The 1BR3 cells were incubated at 37°C in a 5% CO_2 incubator. The medium was changed every 48 hours, and subculturing was performed when the cells reached approximately 80% confluency.

2.5. Internalization of CP-PDEN

Internalization of CP-PDEN was conducted by labeling CP-PDEN with a PKH67 Fluorescent Linker Kit (Sigma-Aldrich, USA), followed by centrifugation at 20000×g for 1 h at 4°C. The supernatant was removed, and the pellet was washed with aquabidest and centrifuged again at 20000×g for 15 min twice at 4°C. The obtained pellet was then resuspended in a serum-free medium. 1BR3 cells were first seeded in glass-bottomed dishes at a density of 1×10^4 cells/dish

and incubated in a complete medium for 24 hours prior to labeling. The medium was then aspirated, and the cells were incubated for 1 hour with PKH67-labeled CP-PDEN. Afterward, the cells were washed with PBS and fixed with 4% paraformaldehyde (Sigma-Aldrich, USA) for 15 minutes and stained with DAPI (Thermo Fisher Scientific, USA) for 10 minutes. Internalization was observed using a confocal fluorescence microscope (Olympus FV-4000) (You *et al*. 2021).

2.6. Cytotoxicity of CP-PDEN

1BR3 cells were seeded in a 96-well plate at a density of 5×10^3 cells/well and incubated in a complete medium for 24 hours. The cells were then treated with varying concentrations of CP-PDEN 2.5, 5, 7.5, and 10 µg/ml and incubated for another 24 hours. After incubation, the medium was aspirated, and 100 µL MTT working reagent (5 µM MTT in serum-free DMEM) was added to each well and incubated at 37°C for 4 hours. The formed formazan crystals were dissolved using 50 µL/well of DMSO. Optical density (OD) was measured using a microplate reader (Bio-Rad) at a wavelength of 595 nm (Mosmann 1983). The percentage of cell viability was calculated as follows:

$$\% \text{ viable cells} = \left(\frac{\text{OD treatments}}{\text{OD untreated controls}} \right) \times 100$$

2.7. UVB Irradiation

1BR3 confluent cells were treated with 2.5 µg/ml and 5 µg/ml CP-PDEN and incubated for 120 minutes at 37°C and 5% CO_2. The cells were then washed with PBS and irradiated with a UVB lamp (Lucky Herp, China) at 100 mJ/cm² in PBS for 15 minutes. After irradiation, PBS was aspirated, and a complete medium was added to the cell cultures, followed by a 24-hour incubation (Deng *et al*. 2018).

2.8. Photoprotective Effect of CP-PDEN on 1BR3 Cells Viability

1BR3 cells were seeded in a 96-well plate at a density of 5×10^3 cells/well and incubated in a complete medium for 24 hours. The cells were then treated with varying concentrations of CP-PDEN and exposed to UVB radiation, followed by a 24-hour incubation. To check the photoprotective effect of CP-PDEN on cell viability, 100 µL of MTT working reagent (5 µM MTT in serum-free DMEM) was added to each well and incubated for 4 hours. The formed formazan crystals were dissolved using 50 µL/well of DMSO. Optical density (OD) was measured using a microplate reader (Bio-Rad) at a wavelength of 595 nm (Deng *et al*. 2018; Zhao *et al*. 2018).

2.9. Photoprotective Effect of CP-PDEN on 1BR3 Cells Nuclear Morphology

1BR3 cells were seeded on sterile cover glasses placed in an 8-well plate at a density of 5×10^4 cells/cover glass and incubated in a complete medium for 48 hours. The cells were then treated with varying concentrations of CP-PDEN and exposed to UVB radiation, followed by a 24-hour incubation. After incubation, the cells were fixed with 4% paraformaldehyde (Sigma-Aldrich, USA) for 15 minutes. The cells were then washed with PBS, and the cell membranes were permeabilized using 0.5% Triton X-100 (Sigma-Aldrich, USA) for 10 minutes, followed by DAPI staining (Thermo Fisher Scientific, USA) for 10 minutes. The cells were washed using PBS, and the cover glasses were mounted on microscope slides with glycerol-PBS (2:1). Then, the cells were closed using cover glass. Cell morphology was observed using a fluorescence microscope (Aird & Zhang 2012).

2.10. Migration Assay of CP-PDEN on 1BR3 Cells

1BR3 cells were seeded in a 24-well plate at a density of 5×10^4 cells/well and incubated in a complete medium for 24 hours. After incubation, the medium was aspirated, and the cells were washed with PBS. A scratch was made in the cell layer of each well using a sterile 100 µL pipette tip. The PBS was then aspirated, and a basic medium containing 2.5 µg/ml and 5 µg/ml CP-PDEN was added. Cell migrations were observed at 8 hours and 24 hours post-treatment using an inverted microscope at 20× magnification (Shu *et al*. 2023).

2.11. Anti-Melanogenesis Effect of CP-PDEN

Male and female zebrafish broodstock were mated (2:1) under constant conditions (16 hours light and 8 hours dark cycle at 28°C). Zebrafish embryos were then transferred from the aquarium to petri dishes using a plastic pipette and washed with sterile deionized water. The embryos were observed under a stereo microscope to separate fertilized from non-fertilized embryos. Zebrafish embryos were then randomly divided into four treatment groups in 24-well plates (8 larvae per well), with each group containing 2 ml of E3 medium (5 mM NaCl, 0.17 mM KCl, 0.33 mM $CaCl_2$, 0.33 mM $MgSO_4$ without methylene blue). The treatment groups were as follows: (1) negative control (no treatment);

(2) positive control using 1-phenyl 2-thiourea (PTU) as a tyrosinase inhibitor; (3) CP-PDEN 2.5 µg/ml in E3 medium; and (4) CP-PDEN 5 µg/ml in E3 medium. The anti-melanogenesis effect was observed by anesthetizing the zebrafish. The fish were positioned ventral side up and observed at 72 hours, 96 hours, and 120 hours using a stereo microscope (Zeiss Stemi 508). Pigmentation changes in the zebrafish were analyzed using ImageJ software (Kusnandar *et al*. 2024).

2.12. Statistical Analysis

The results are reported as mean ± standard deviation (SD), n≥3. Data was analyzed using one-way ANOVA, with a p-value<0.05 was considered statistically significant. Statistical analysis was performed using GraphPad Prism software (GraphPad Software, Inc.).

3. Results

3.1. Characterization of CP-PDEN

Papaya-derived exosome-like nanoparticles (CP-PDEN) were isolated using a differential centrifugation and precipitation method with polyethylene glycol 6000 (PEG6000). The size distribution analysis of CP-PDEN revealed nanoparticle diameters ranging from 105.10-218.60 nm, with an average diameter of 135.4±0.15 nm. Moreover, the zeta potential analysis showed that the nanoparticles were negatively charged and had an average zeta potential of -17.03±0.2 mV. Furthermore, morphological visualization of CP-PDEN using low-resolution transmission electron microscopy (LR-TEM) (Figure 1) confirmed a spherical shape with protein concentration, as measured by the bicinchoninic acid (BCA) assay, revealed an average CP-PDEN protein concentration of 1492±96 µg/ml.

3.2. Internalization of CP-PDEN

The internalization assay was conducted to determine the time required for CP-PDEN to enter 1BR3 cells, a human fibroblast cell line with elongated and spindle-shaped morphology (Figure 2A). In this study, CP-PDEN was labeled with the fluorescent dye PKH67 (green), which is commonly used for labeling mammalian exosomes. Additionally, DAPI staining was performed to label the nucleus. Confocal microscopy observations (Figure 2B) revealed that CP-PDEN was internalized into 1BR3 cells within 1 hour.

3.3. Cytotoxicity of CP-PDEN

The cytotoxicity of CP-PDEN was assessed by exposing 1BR3 cells to varying concentrations of CP-PDEN for 24 hours, followed by the administration of an MTT reagent. The results (Figure 3) indicated that CP-PDEN at concentrations of 2.5 µg/ml and 5 µg/ml did not show a significant reduction in cell viability (p>0.05) compared to the control. According to ISO 10993-5 (2009), cell viability above 80% is considered non-cytotoxic. Therefore, CP-PDEN concentrations of 2.5 µg/ml and

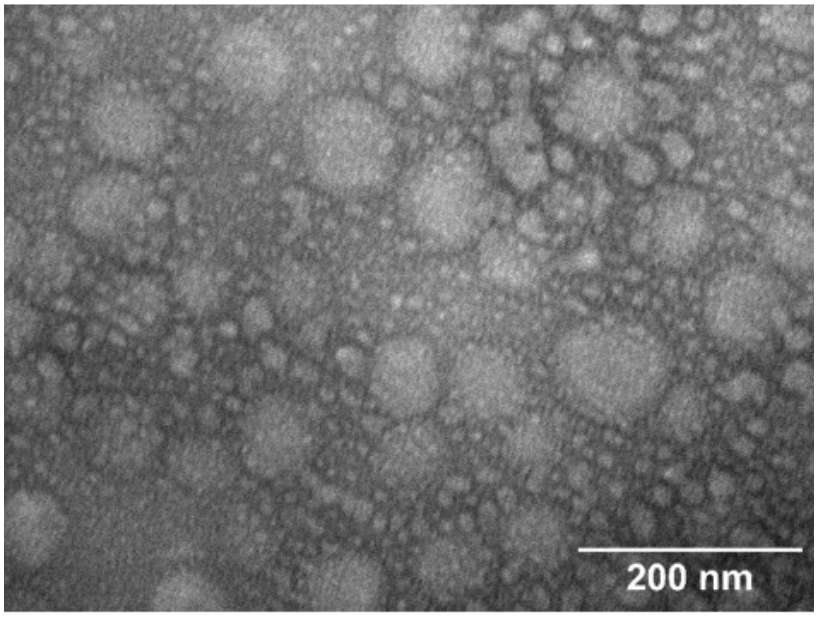

Figure 1. Visualization of CP-PDEN morphology using low-resolution transmission electron microscopy (LR-TEM)

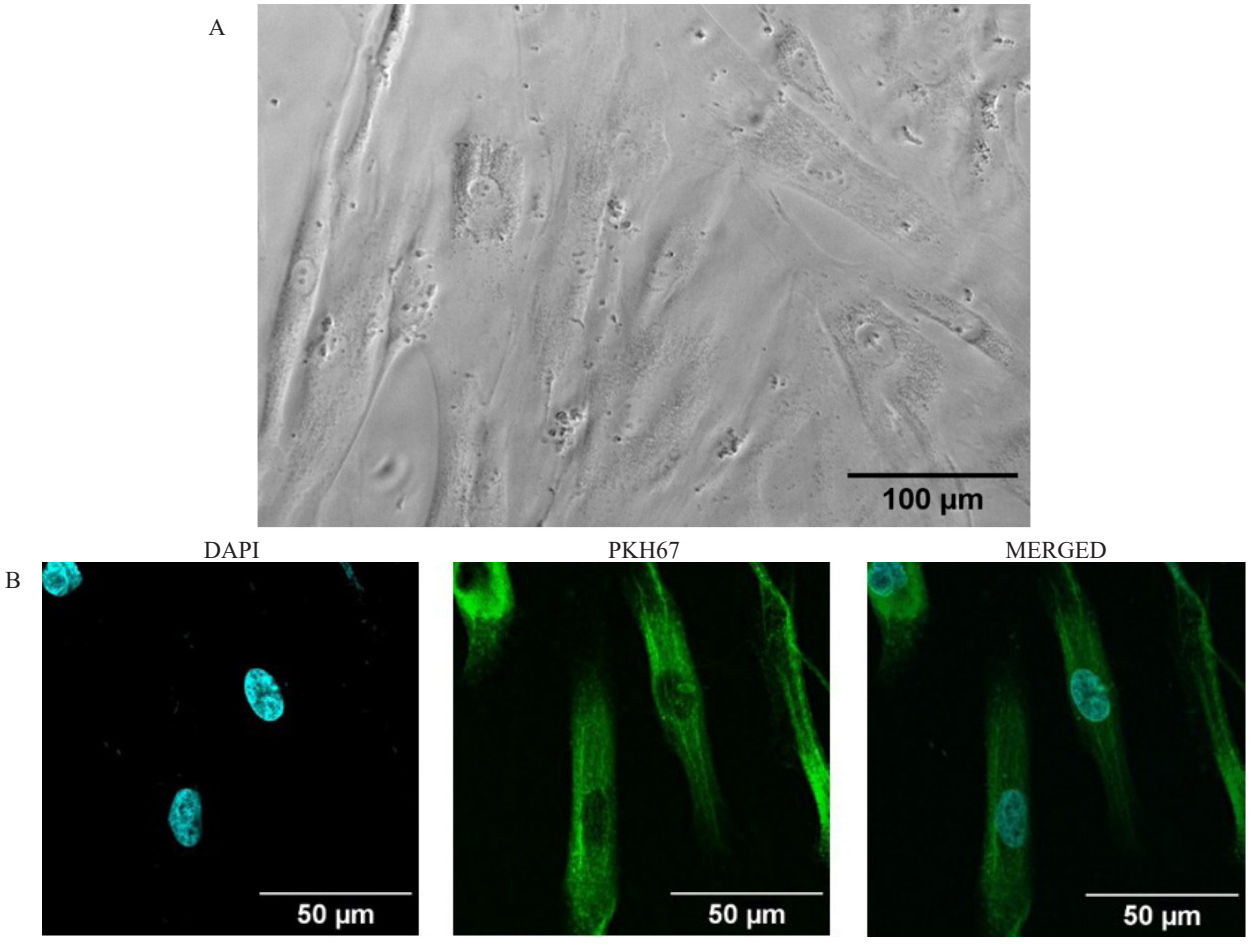

Figure 2. (A) Morphology of 1BR3 cells under inverted microscope (100× magnification), (B) Internalization of CP-PDEN in 1BR3 cells using PKH67 staining under a confocal fluorescence microscope (100× magnification)

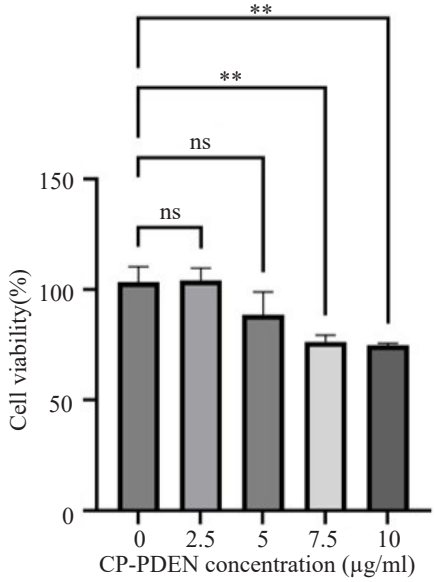

Figure 3. Cytotoxic assay of CP-PDEN in 1BR3 cells using MTT assay

5 µg/ml, with respective cell viabilities of 104.14% and 88.54%, are classified as non-toxic.

3.4. Photoprotective Effect of CP-PDEN on 1BR3 Cells Viability

The photoprotective effects of CP-PDEN on 1BR3 cells were assessed by measuring cell viability after treatment with varying concentrations of CP-PDEN and exposure to UVB irradiation at 100 mJ/cm². The results (Figure 4) demonstrated that treatment with 2.5 µg/ml CP-PDEN significantly increased 1BR3 cell viability ($p<0.05$) following UVB exposure. Compared to UVB-exposed cells without CP-PDEN treatment, which had a viability of 65.32%, there was an approximate 19% increase in viability to 84.11%. Meanwhile, treatment with 5 µg/ml CP-PDEN also increased cell viability by approximately 11% to 76.34%, though this was not statistically significant ($p>0.05$). The reduction in cell viability following UVB exposure is likely due to increased DNA damage and ROS production induced by UVB.

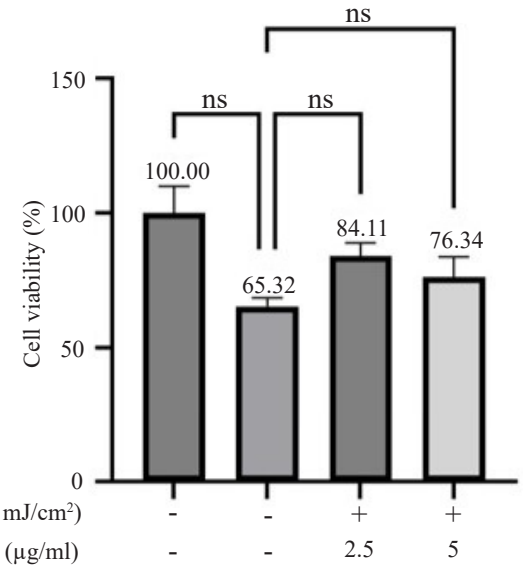

Figure 4. Photoprotective effect of CP-PDEN in 1BR3 cells viability using MTT assay

3.5. Photoprotective Effect of CP-PDEN on 1BR3 Cells Nuclear Morphology

Evaluation of nuclear morphology changes in 1BR3 cells following UVB irradiation and CP-PDEN treatment was performed using DAPI staining. Visualization of the 1BR3 nuclei post-staining is shown in (Figure 5). The results indicated that UVB-irradiated cells without CP-PDEN treatment exhibited uneven staining, with some areas showing higher fluorescence intensity and an enlarged nuclear size compared to the control. In contrast, cells treated with 2.5 µg/ml CP-PDEN displayed more uniform nuclear staining and no nuclear enlargement. Cells treated with 5 µg/ml CP-PDEN showed some areas of higher fluorescence intensity, though nuclear enlargement was not observed.

3.6. Effect of CP-PDEN on 1BR3 Cells Migration Activity

The migration activity of 1BR3 fibroblast cells was evaluated using the scratch assay method. As shown in (Figure 6), the wound closure area increased over time.

Quantification and statistical analysis of the wound closure area were conducted to assess the effect of CP-PDEN treatment on cell migration. The results (Figure 7) demonstrated that treatment with 2.5 µg/ml CP-PDEN significantly increased the wound closure area ($p<0.05$) compared to the control at both 8 and 24 hours. However, treatment with 5 µg/ml CP-PDEN did not result in a significant increase in wound closure area ($p>0.05$) compared to the control at either time point.

3.7. Anti-Melanogenesis Effect of CP-PDEN

The in vivo testing of CP-PDEN was conducted on zebrafish (*Danio rerio*) to evaluate its effects on melanogenesis activity. PTU (1-phenyl 2-thiourea) was used as a positive control due to its role as a tyrosinase inhibitor. Visual observations (Figure 7A) showed that treatment with 2.5 µg/ml and 5 µg/ml CP-PDEN resulted in more transparent zebrafish bodies.

To confirm the effect of CP-PDEN on anti-melanogenesis activity, quantification and statistical analysis of melanocyte counts were performed. The analysis (Figure 7B) revealed that treatment with 2.5 µg/ml CP-PDEN significantly suppressed melanogenesis ($p<0.05$) compared to PTU as the positive control. Meanwhile, treatment with 5 µg/ml CP-PDEN also reduced melanogenesis, though not significantly ($p>0.05$), compared to PTU. It was noted that the reduction in melanocyte numbers occurred consistently rather than gradually across all observation times.

4. Discussion

In this study, papaya-derived exosome-like nanoparticles (CP-PDEN) were isolated using differential centrifugation and precipitation method with polyethylene glycol 6000 (PEG6000). The result showed that this isolation method generates a spherical shape CP-PDEN with an average diameter of 135.4±0.15 nm and an average zeta potential of -17.03±0.2 mV, aligning with earlier findings (Iriawati *et al*. 2024). These findings corroborate the reproducibility of CP-PDEN characteristics, supporting the reliability of the PEG6000 precipitation method for isolating PDEN with consistent size, charge, and morphology.

Our study also confirmed that CP-PDEN could be internalized into 1BR3 cells within 1 hour. Previous research on CP-PDEN internalization in RAW 264.7 macrophage cells indicated that it took 2 hours for CP-PDEN to be internalized (Iriawati *et al*. 2024). In general, PDEN internalization is thought to occur through three main pathways: membrane fusion, endocytosis, and macropinocytosis (Zhang *et al*. 2022). In this study, CP-PDEN likely entered 1BR3 cells via the endocytosis pathway. Nanoparticles with sizes ranging from 100-200 nm are known to internalize through clathrin-mediated endocytosis, which supports particles within this size range (Rejman *et al*. 2004). In contrast, other studies involving grape-derived exosome-like nanoparticles (GrDEN) showed internalization was found to occur through macropinocytosis (Ju *et al*.

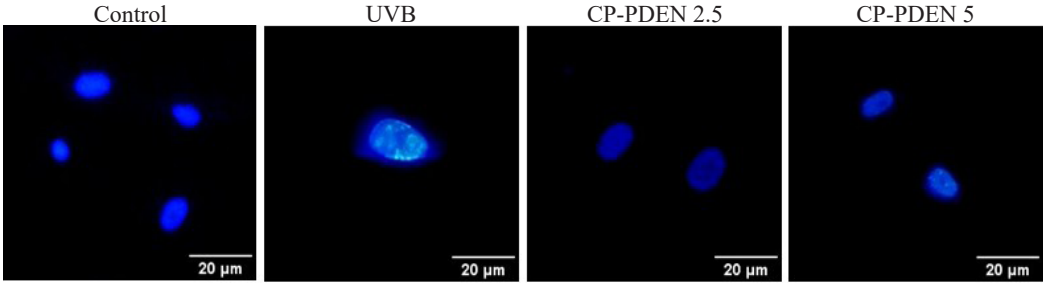

Figure 5. Photoprotective effect of CP-PDEN in 1BR3 cells nuclear morphology using DAPI staining under a fluorescence microscope (40× magnification)

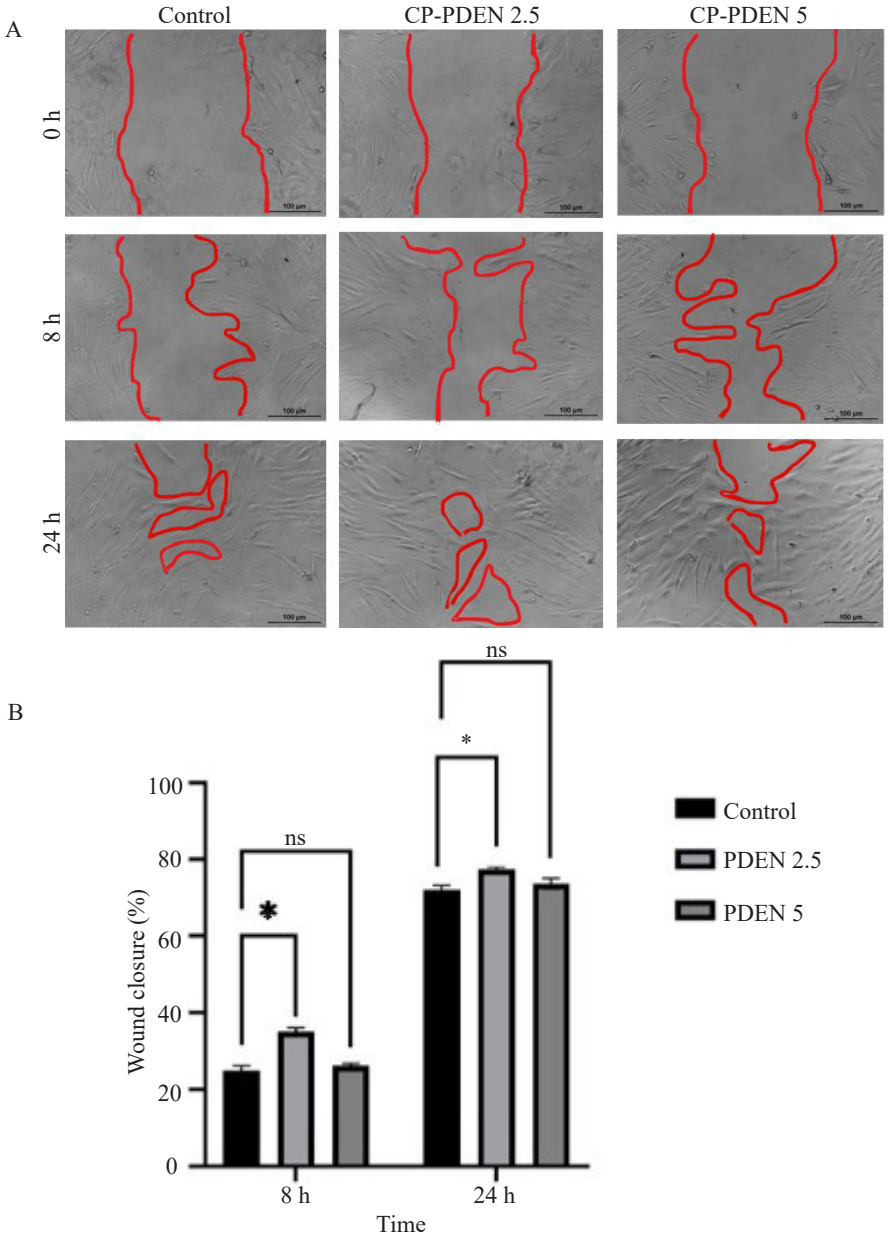

Figure 6. (A) Visualization of 1BR3 cell migration activity using the scratch assay method under an inverted microscope (40× magnification), (B) Quantification of the wound closure area in 1BR3 cells using ImageJ

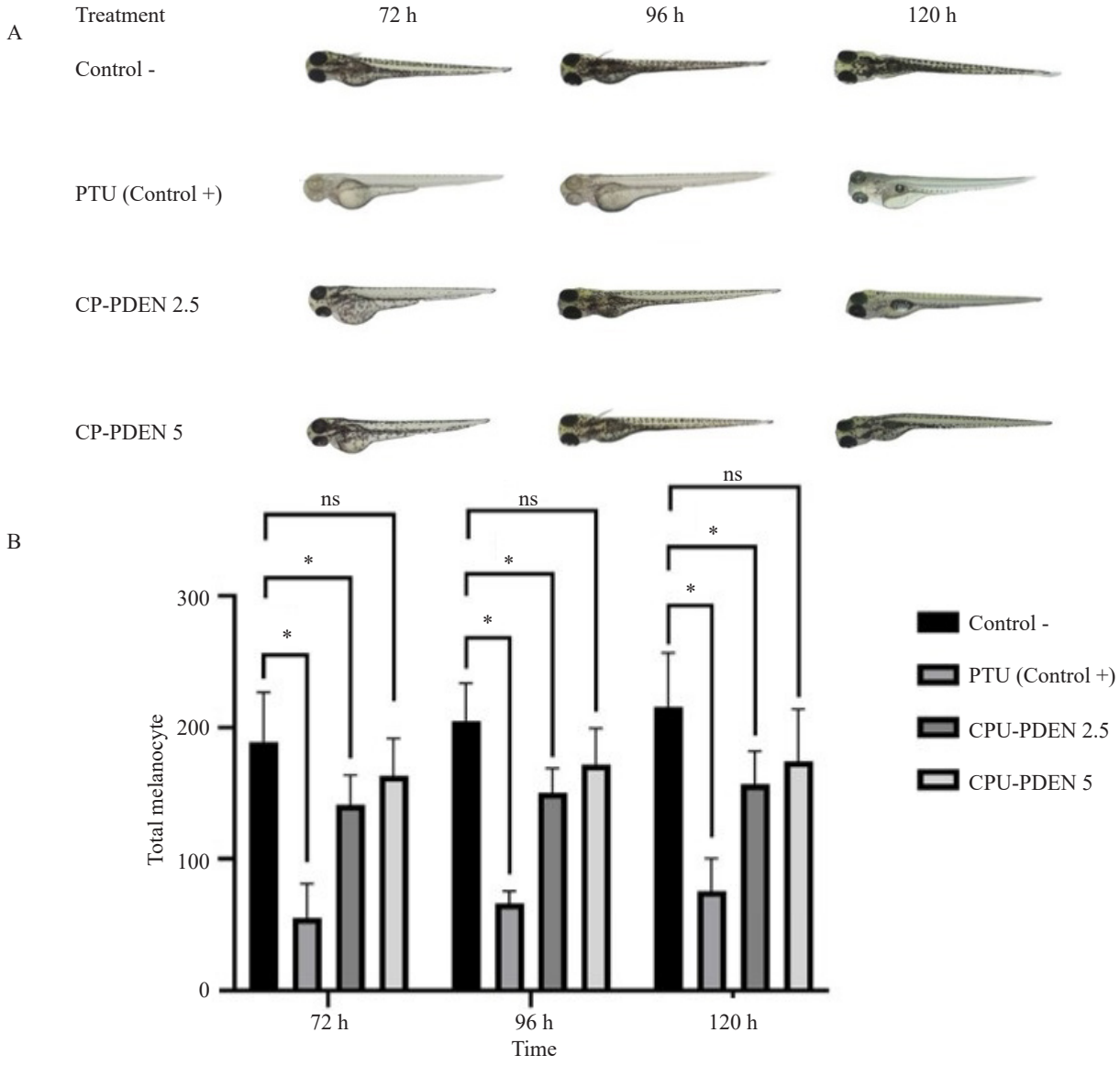

Figure 7. (A) Visual observations of CP-PDEN anti-melanogenesis effect on zebrafish under stereo microscope, (B) Quantification of zebrafish melanocyte counts ImageJ

2013). These variations in internalization pathways are likely due to differences in membrane proteins, which facilitate different internalization routes (Zhang *et al*. 2022).

After investigating the CP-PDEN physical characteristics and its uptake, we also tested its toxicity on 1BR3 cells. The result showed CP-PDEN concentrations of 2.5 µg/ml and 5 µg/ml, with respective cell viabilities of 104.14% and 88.54%, are classified as non-toxic, according to ISO 10993-5 (2009), which stated that cell viability above 80% is considered non-cytotoxic. The cytotoxicity levels may vary depending on the target cells and the source of PDEN. A previous study assessing CP-PDEN cytotoxicity in RAW 264.7 macrophage cells demonstrated that concentrations up to 100 µg/ml were still non-toxic (Iriawati *et al*. 2024). This variation in cytotoxicity levels may be attributed to the fact that macrophages are immune cells with detoxification mechanisms, which increase their resistance to cytotoxic compounds (Ben *et al*. 2013).

Next, we examined the photoprotective effect of CP-PDEN on UVB-irradiated 1BR3 cells viability. The results demonstrated that 2,5 µg/ml CP-PDEN significantly increased 1BR3 cell viability following UVB exposure. Previous studies using the same UVB dose (100 mJ/cm²) on fibroblasts reported a similar decrease in viability of about 30% compared to control, along with elevated cellular markers of photoaging, such

as increased ROS production, β-galactosidase activity, and the proportion of cells arrested at the G2 phase of the cell cycle (Deng *et al*. 2018). The G2/M checkpoint itself is known to prevent mitosis in cells with DNA damage during the G2 phase (Lukas *et al*. 2004). One of the key bioactive compounds in CP-PDEN, maltol, has known antioxidant properties that help inhibit UVB-induced cellular apoptosis and senescence. Maltol suppresses ROS production by enhancing the activity of natural antioxidants like superoxide dismutase (SOD), which reduces malondialdehyde (MDA), a byproduct of lipid peroxidation. Moreover, maltol facilitates the translocation of the transcription factor nuclear respiratory factor-2 (Nrf-2) to the nucleus, promoting the expression of heme oxygenase-1 (HO-1) (Sha *et al*. 2019). The Nrf-2 pathway is one of the primary mechanisms of the body's natural antioxidant defense. Activation of this pathway upregulates cytoprotective and antioxidant genes, including HO-1, which can inhibit the production of pro-inflammatory cytokines such as IL-1β, IL-6, and TNF-α (Paine *et al*. 2010).

Furthermore, we evaluated the nuclear morphology changes in 1BR3 cells following UVB irradiation and CP-PDEN treatment using DAPI staining. The results indicated that cells treated with CP-PDEN displayed more uniform nuclear staining and no nuclear enlargement. In general, senescent cells are characterized by an enlarged nucleus, thought to be caused by cell cycle arrest in the G1 or G2 phase, leading to intracellular content accumulation for cell division, which results in nuclear enlargement (Huang *et al*. 2022). Moreover, senescent cells often exhibit brighter regions within the nucleus, known as senescence-associated heterochromatin foci (SAHF). SAHF arises due to heterochromatin condensation that suppresses the expression of proliferation-associated genes like E2F, explaining the inhibited proliferative activity observed in senescent cells (Aird & Zhang 2012). One of the bioactive compounds in CP-PDEN, maltol, has been shown to inhibit cellular senescence by suppressing the expression of p53 and p21 proteins, which are involved in cell cycle arrest through inhibition of cyclin-CDK complex activity (Sha *et al*. 2021). Additionally, CP-PDEN has also been reported to reduce the production of interleukin-6 (IL-6), a pro-inflammatory cytokine and part of the senescence-associated secretory phenotype (SASP). SASP can induce paracrine senescence, exacerbating the spread of senescent cells within a tissue (Huang *et al*. 2022; Iriawati *et al*. 2024).

We also evaluated the migration activity of 1BR3 fibroblast cells using the scratch assay method. The results demonstrated that 2.5 µg/ml CP-PDEN significantly increased the wound closure area compared to the control. Cell migration plays a critical role in tissue regeneration following UVB-induced skin damage. Apoptotic cells are eliminated from the skin tissue via an inflammatory response that induces the secretion of pro-inflammatory cytokines such as IL-1β, IL-6, and TNF-α. These cytokines are involved in recruiting immune cells to remove apoptotic debris and recruiting growth factors such as FGF and PDGF, which induce activation and proliferation of fibroblasts, leading to tissue regeneration (Mahmoud *et al*. 2024). Previous studies have shown that CP-PDEN can enhance the secretion of the anti-inflammatory cytokine IL-10, which plays a role in upregulating the synthesis of extracellular matrix components such as COL-1 (Iriawati *et al*. 2024). The interaction between COL-1 and fibroblast cells through integrin receptors is known to activate signaling pathways that promote cell proliferation (Elango *et al*. 2022). Another study also revealed that one of the bioactive compounds in CP-PDEN, maltol, can increase the production of the anti-inflammatory cytokine TGF-β, which is involved in inducing fibroblast migration and proliferation (Kong *et al*. 2021).

The in vivo testing of CP-PDEN was conducted on zebrafish (*Danio rerio*) to evaluate its effects on melanogenesis activity. PTU (1-phenyl 2-thiourea) was used as a positive control due to its role as a tyrosinase inhibitor. The result revealed that 2.5 µg/ml CP-PDEN significantly suppressed melanogenesis compared to PTU as the positive control. Various external factors, including UVB radiation can influence melanin production by melanocytes. Extreme levels of UVB can increase melanin production, particularly eumelanin, leading to hyperpigmentation as a marker of photoaging. This occurs because melanin protects the skin from UVB by absorbing and reducing its penetration into deeper layers of the skin (Yardman-Frank & Fisher 2021). In this study, the anti-melanogenesis activity observed with CP-PDEN treatment may be due to its ability to reduce IL-1β secretion (Iriawati *et al*. 2024). Previous studies have shown that IL-1β plays a role in increasing the expression of tyrosinase (TYR) and tyrosinase-related protein-1 (TRP-1), which are key enzymes in the melanogenesis process (Yang *et al*. 2022). This hypothesis is further supported by research indicating that one of the bioactive compounds in CP-

PDEN, maltol, can reduce the expression of TYR and TRP-1 (Han *et al*. 2023). As a nanocosmetic agent, PDEN offers a reversible effect, which is necessary to prevent long-term side effects and permanent inhibition of melanogenesis (Kusnandar *et al*. 2024).

The insignificant results observed in CP-PDEN at a concentration of 5 µg/ml may be attributed to nonlinear pharmacokinetic behavior, where an increase in dose does not produce a linear effect due to drug saturation (Shargel & Yu 2016). This phenomenon was also observed in a previous study using CP-PDEN, where the results do not follow a dose-dependent manner (Iriawati *et al*. 2024). However, further research is needed to fully elucidate the mechanisms underlying this behavior of CP-PDEN.

Acknowledgements

The authors would like to thank ITB Olympus Bioimaging Centre (IOBC) for providing access to the confocal scanning microscope.

References

Aird, K. M., Zhang, R., 2012. Detection of senescence-associated heterochromatin foci (SAHF). *Methods Mol Biol*. 965, 185-96. https://doi.org/10.1007/978-1-62703-239-1_12

Ben, J., Zhang, Y., Zhou, R., Zhang, H., Zhu, X., Li, X., Zhang, H., Li, N., Zhou, X., Bai, H., Yang, Q., Li, D., Xu, Y., Chen, Q., 2013. Major vault protein regulates class A scavenger receptor-mediated tumor necrosis factor-α synthesis and apoptosis in macrophages. *J Biol Chem*. 288, 20076-20084. https://doi.org/10.1074/jbc.M112.449538

Calvo, M.J., Navarro, C., Durán, P., Galan-Freyle, N.J., Parra Hernández, L.A., Pacheco-Londoño, L.C., Castelanich, D., Bermúdez, V., Chacin, M., 2024. Antioxidants in Photoaging: From Molecular Insights to Clinical Applications. *Int J Mol Sci*. 25, 2403. https://doi.org/10.3390/ijms25042403

Deng, M., Li, D., Zhang, Y., Zhou, G., Liu, W., Cao, Y., Zhang, W. 2018. Protective effect of crocin on ultraviolet B induced dermal fibroblast photoaging. *Mol Med Rep*. 18, 1439-1446. https://doi.org/10.3892/mmr.2018.9150

Elango, J., Hou, C., Bao, B., Wang, S., Maté Sánchez de Val, J.E., Wenhui, W., 2022. The molecular interaction of collagen with cell receptors for biological function. *Polymers* (Basel). 14, 876. https://doi.org/10.3390/polym14050876

Han, N.R., Park, H.J., Ko, S.G., Moon, P.D., 2023. Maltol has anti-cancer effects via modulating PD-L1 signaling pathway in B16F10 cells. *Front Pharmacol*. 14, 1255586. https://doi.org/10.3389/fphar.2023.1255586

Huang, W., Hickson, L.J., Eirin, A., Kirkland, J.L., Lerman, L.O., 2022. Cellular senescence: the good, the bad and the unknown. *Nat Rev Nephrol*. 18, 611-627. https://doi.org/10.1038/s41581-022-00601-z

Iriawati, I., Vitasasti, S., Rahmadian, F.N.A., Barlian, A., 2024. Isolation and characterization of plant-derived exosome-like nanoparticles from *Carica papaya* L. fruit and their potential as anti-inflammatory agent. *PLoS One*. 19, e0304335. https://doi.org/10.1371/journal.pone.0304335

ISO 10993-5., 2009. Biological evaluation of medical devices-part 5: tests for in vitro cytotoxicity. International Organization for Standardization.

Ju, S., Mu, J., Dokland, T., Zhuang, X., Wang, Q., Jiang, H., Xiang, X., Deng, Z.B., Wang, B., Zhang, L., Roth, M., Welti, R., Mobley, J., Jun, Y., Miller, D., Zhang, H.G., 2013. Grape exosome-like nanoparticles induce intestinal stem cells and protect mice from DSS-induced colitis. *Mol Ther.* 21, 1345-1357. https://doi.org/10.1038/mt.2013.64

Kong, Y.R., Jong, Y.X., Balakrishnan, M., Bok, Z.K., Weng, J.K. K., Tay, K.C., Goh, B.H., Ong, Y.S., Chan, K.G., Lee, L.H., Khaw, K.Y., 2021. Beneficial role of *Carica papaya* extracts and phytochemicals on oxidative stress and related diseases: A mini review. *Biology* (Basel). 10, 287. https://doi.org/10.3390/biology10040287

Kusnandar, M.R., Wibowo, I., Barlian, A., 2024. Characterizing nanoparticle isolated by yam bean (*Pachyrhizus erosus*) as a potential agent for nanocosmetics: An *in vitro* and *in vivo* approaches. *Pharm Nanotechnol*. 13, 341-357. https://doi.org/10.2174/0122117385279809231221050226

Lukas, J., Lukas, C., Bartek, J., 2004. Mammalian cell cycle checkpoints: signalling pathways and their organization in space and time. *DNA Repair* (Amst). 3, 997-1007. https://doi.org/10.1016/j.dnarep.2004.03.006

Mahmoud, N.N., Hamad, K., Al Shibitini, A., Juma, S., Sharifi, S., Gould, L., Mahmoudi, M., 2024. Investigating inflammatory markers in wound healing: Understanding implications and identifying artifacts. *ACS Pharmacol Transl Sci*. 7, 18-27. https://doi.org/10.1021/acsptsci.3c00336

Mosmann, T., 1983. Rapid colorimetric assay for cellular growth and survival: application to proliferation and cytotoxicity assays. *J Immunol Methods*. 65, 55-63. https://doi.org/10.1016/0022-1759(83)90303-4

Paine, A., Eiz-Vesper, B., Blasczyk, R., Immenschuh, S., 2010. Signaling to heme oxygenase-1 and its anti-inflammatory therapeutic potential. *Biochem Pharmacol*. 80, 1895-1903. https://doi.org/10.1016/j.bcp.2010.07.014

Pandel, R., Poljšak, B., Godic, A., Dahmane, R., 2013. Skin photoaging and the role of antioxidants in its prevention. *ISRN Dermatol*. 2013, 930164. https://doi.org/10.1155/2013/930164

Rejman, J., Oberle, V., Zuhorn, I.S., Hoekstra, D., 2004. Size-dependent internalization of particles via the pathways of clathrin- and caveolae-mediated endocytosis. *Biochem J.* 377, 159-169. https://doi.org/10.1042/bj20031253

Sall, I.M., Flaviu, T.A., 2023. Plant and mammalian-derived extracellular vesicles: a new therapeutic approach for the future. *Front Bioeng Biotechnol*. 11, 1215650. https://doi.org/10.3389/fbioe.2023.1215650

Sarasati, A., Syahruddin, M.H., Nuryanti, A., Ana, I.D., Barlian, A., Wijaya, C.H., Ratnadewi, D., Wungu, T.D.K., Takemori, H., 2023. Plant-derived exosome-like nanoparticles for biomedical applications and regenerative therapy. *Biomedicines*. 11, 1053. https://doi.org/10.3390/biomedicines11041053

Sha, J.Y., Zhou, Y.D., Yang, J.Y., Leng, J., Li, J.H., Hu, J.N., Liu, W., Jiang, S., Wang, Y.P., Chen, C., Li, W., 2019. Maltol (3-hydroxy-2-methyl-4-pyrone) slows D-galactose-induced brain aging process by damping the Nrf2/HO-1-mediated oxidative stress in mice. *J Agric Food Chem*. 67 10342-10351. https://doi.org/10.1021/acs.jafc.9b04614

Sha, J.Y., Li, J.H., Zhou, Y.D., Yang, J.Y., Liu, W., Jiang, S., Wang, Y.P., Zhang, R., Di, P., Li, W., 2021. The p53/p21/p16 and PI3K/Akt signaling pathways are involved in the ameliorative effects of maltol on D-galactose-induced liver and kidney aging and injury. *Phytother Res*. 35, 4411–4424. https://doi.org/10.1002/ptr.7142

Shargel, L., Yu, A.B.C., 2016. *Applied Biopharmaceutics & Pharmacokinetics,* McGraw Hill Education, New York.

Shu, P., Li, M., Zhao, N., Wang, Y., Zhang, L., Du, Z., 2023. Efficacy and mechanism of retinyl palmitate against UVB-induced skin photoaging. *Front Pharmacol*. 14, 1278838. https://doi.org/10.3389/fphar.2023.1278838

Yang, C.Y., Guo, Y., Wu, W.J., Man, M.Q., Tu, Y., He, L., 2022. UVB-induced secretion of IL-1β promotes melanogenesis by upregulating TYR/TRP-1 expression *In Vitro*. *Biomed Res Int*. 2022, 8230646. https://doi.org/10.1155/2022/8230646

Yardman-Frank, J.M., Fisher, D.E., 2021. Skin pigmentation and its control: From ultraviolet radiation to stem cells. *Exp Dermatol*. 30, 560-571. https://doi.org/10.1111/exd.14260

Yi, Q., Xu, Z., Thakur, A., Zhang, K., Liang, Q., Liu, Y., Yan, Y. 2023. Current understanding of plant-derived exosome-like nanoparticles in regulating the inflammatory response and immune system microenvironment. *Pharmacol Res*. 190, 106733. https://doi.org/10.1016/j.phrs.2023.106733

You, J.Y., Kang, S.J., Rhee, W.J., 2021. Isolation of cabbage exosome-like nanovesicles and investigation of their biological activities in human cells. *Bioact Mater*. 6, 4321-4332. https://doi.org/10.1016/j.bioactmat.2021.04.023

Zhang, Z., Yu, Y., Zhu, G., Zeng, L., Xu, S., Cheng, H., Ouyang, Z., Chen, J., Pathak, J.L., Wu, L., Yu, L., 2022. The emerging role of plant-derived exosomes-like nanoparticles in immune regulation and periodontitis treatment. *Front Immunol*. 13, 896745. https://doi.org/10.3389/fimmu.2022.896745

Zhao, P., Alam, M.B., Lee, S.H., 2018. Protection of UVB-induced photoaging by fuzhuan-brick tea aqueous extract via MAPKs/Nrf2-Mediated down-regulation of MMP-1. *Nutrients*. 11, 60. https://doi.org/10.3390/nu11010060